ACS Partner Journal

Journal of the American Society for Mass Spectrometry

pubs.acs.org/jasms

Research Article

Collision Cross-Section Measurements of Collision-Induced Dissociation Precursor and Product Ions in an FTICR-MS and an IM-MS: A Comparative Study

Andrew J. Arslanian, Noah Mismash, and David V. Dearden*

Cite This: J. Am. Soc. Mass Spectrom. 2022, 33, 1626−1635

Read Online

ACCESS | Metrics & More | Article Recommendations | Supporting Information

ABSTRACT: Sustained off-resonance irradiation-cross-sectional areas by Fourier transform ion cyclotron resonance mass spectrometry (SORI-CRAFTI) is an FTICR-MS strategy to collisionally activate precursor ions and then measure their ion-neutral collision cross sections, as well as those of selected products, at the same time. We benchmarked SORI-CRAFTI using protonated leucine-enkephalin, to excellent agreement (typically within 1−2%) with previous studies performed via collision-induced dissociation-ion mobility (CID-IMS). SORI-CRAFTI was then applied to alkali metal-cationized leucine-enkephalin and compared with CID-IMS via precursor/product cross-section ratios. Qualitative agreement between SORI-CRAFTI and CID-IMS was excellent (again, usually within 1−2%); however, neither SORI-CRAFTI nor CID-IMS could determine if metalated leucine-enkephalin was present in its canonical or zwitterionic form. When SORI-CRAFTI was used on [2.2.2]-cryptand+Cs^+, SORI activation resulted in a 5% decrease in collision cross section, consistent with migration of the externally bound Cs^+ into the cryptand's cavity and similar to the cross section observed when electrospraying from an isopropanol-rich solvent. Thus, SORI-CRAFTI is useful for studying gas-phase ion chemistry of small- to medium-sized molecules and host−guest systems.

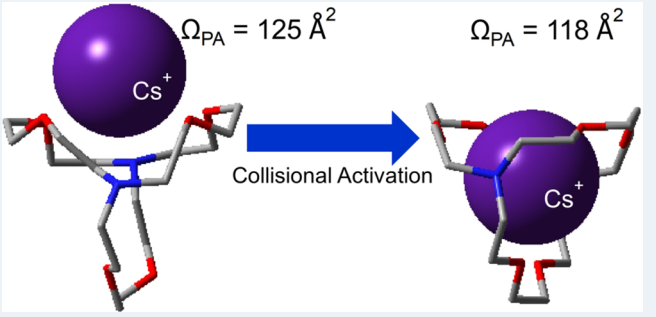

INTRODUCTION

The use of cross-sectional areas by Fourier transform ion cyclotron resonance mass spectrometry (CRAFTI) is a strategy to measure ion-neutral collision cross sections without a dedicated ion mobility instrument, requiring only minimal modification of an existing Fourier transform ion cyclotron resonance mass spectrometer (FTICR-MS).[1] CRAFTI measures ion-neutral collision cross sections through the pressure-limited frequency peak broadening that occurs due to ion-neutral collisions.[2,3] After obtaining multiple mass spectra at various pressures (typically spanning 1 order of magnitude), the target frequency peak's variation in full-width at half-maximum (fwhm) as a function of collision gas pressure is extracted and used to calculate the ion-neutral collision cross section, σ:[3]

$$\sigma = \frac{\text{fwhm}}{N}\frac{m_{\text{ion}}}{q}\frac{\pi d}{\beta V_{\text{pp}} t_{\text{exc}}} \quad (1)$$

Here, fwhm is the frequency peak's full-width at half-maximum, N is the neutral number density, m_{ion} is the ion's mass, d is the trapping cell diameter (0.06 m for our Bruker Infinity cell), β is the trapping cell geometry factor (0.897 for the Bruker Infinity cell),[4] V_{pp} is the peak-to-peak excite amplitude, and t_{exc} is the duration of the excite pulse. Since m_{ion}, q, β, N, d, V_{pp}, and t_{exc} are known, controlled, or otherwise directly measured experimental variables, the purpose of CRAFTI experiments is to measure fwhm and thus determine σ.

Because the FTICR-MS is a capable single-instrument chemical laboratory, CRAFTI can be coupled to premeasurement ion activation strategies with relative ease. Such coupling might allow σ measurement after collision-induced dissociation, collision-induced unfolding, chemical reactions, etc. and might provide additional structural information available after ion activation. Such information could include cross-sectional size of product ions, protein size after collisional unfolding, or the time-dependent size of ions formed through chemical reactions. One purpose of this paper is to demonstrate the feasibility of the SORI-CRAFTI approach and to benchmark it against more conventional IMS-based ion activation-mobility measurement techniques. While this paper focuses on SORI-

Received: March 28, 2022
Revised: June 29, 2022
Accepted: July 20, 2022
Published: July 27, 2022

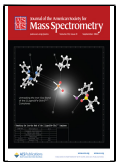

Scheme 1

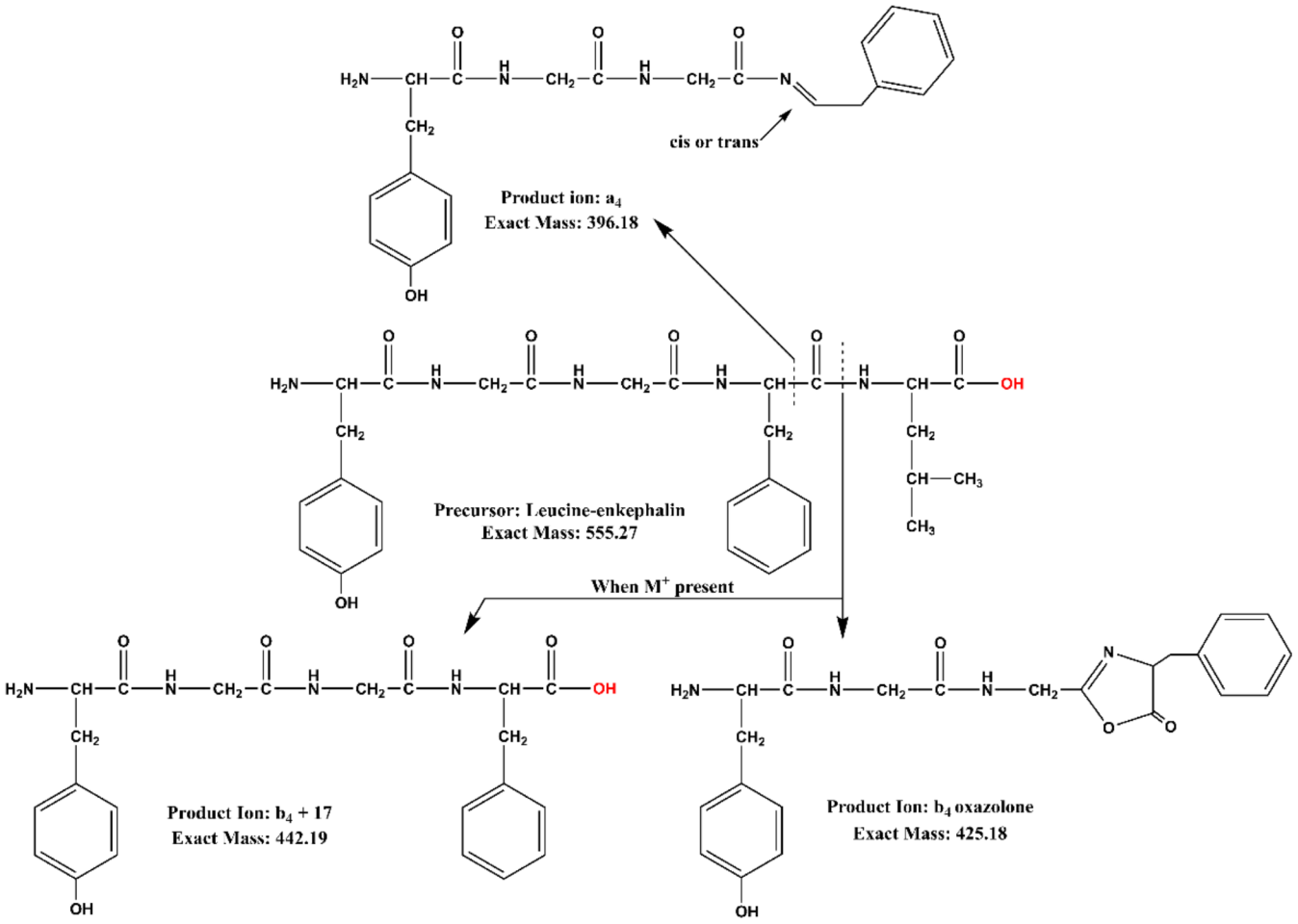

CRAFTI, additional "ion activation-CRAFTI" strategies are also expected to work.

SORI-CRAFTI analyzes precursor and product ions in the same experiment by measuring their ion-neutral σ. This is accomplished by first dissociating the precursor ion through sustained off-resonance irradiation collision-induced dissociation (SORI-CID) and then simultaneously exciting the precursor and a selected product ion for σ measurements. By performing the experiments in this fashion, the relative σ of precursor and product(s) can be directly compared under identical pressures, and the products can be compared against each other. Such experimental design may lead to details about gas-phase ion structure unavailable by other means.

To benchmark this technique, leucine-enkephalin (LE), as seen in Scheme 1, was used because it is a common mass spectrometry standard.[5] Proof-of-concept work focused on LE $+H^+$ since its gas-phase dissociation chemistry has been extensively characterized by tandem mass spectrometry (as reviewed in ref 5), the precursor and some products have been characterized using infrared spectroscopy,[6] and the cold precursor has been characterized using both ultraviolet and infrared spectroscopy.[7] The numerous tandem mass spectrometry studies reveal that LE$+H^+$ dissociates through water loss, b_n, a_n, and y_n product channels and that the products obtained depend on energy during collision-induced dissociation. Polfer et al.[6] determined that the n-terminus is LE's most probable protonation site, that the b_4 fragment (Scheme 1) has an oxazolone structure that can cyclize then undergo ring opening to rearrange the sequence, and that the a_4 structure (Scheme 1) possesses an imine trans double bond between the fourth amine (numbered from the *n*-terminus) and the phenylalanine side chain. In both the b_4 and a_4 structures, the *n*-terminus is protonated and solvated by the carbonyl backbone. Burke et al.[7] reached slightly different conclusions about the low energy structure adopted by LE$+H^+$, specifically with regard to intramolecular interactions present around the c-terminus. The structural differences were attributed to the fact that the Polfer study was at room temperature while the Burke study was performed on cold (25−110 K) LE. A delightful takeaway from the Burke study is that the experimentally determined LE $+H^+$ structure has a conformational size in agreement with rotationally averaged momentum transfer cross-section measurements obtained through ion mobility.[8,9] The information from the Polfer[6] and Burke[7] papers was highly valuable to us in benchmarking SORI-CRAFTI with LE$+H^+$, and its fragments.

In the face of such detailed information about leucine-enkephalin, the dearth of studies related to the metal cationized peptide is surprising. A 2011 review[5] relates just two articles which describe LE$+Na^+$ fragmentation. That entire discussion comprises one-half of one column of a review that is 22 pages in length. Two additional studies published in the late 1980s discuss LE$+M^+$ fragmentation where M^+ is Li^+, Na^+, or K^+.[10,11] These studies, which differ in the precursor structure (canonical vs zwitterion) reveal that collisionally activated LE $+M^+$ dissociates to form b_n+17+M^+ ions (Scheme 1), where 17 corresponds to an additional −OH group on the new c-

https://doi.org/10.1021/jasms.2c00089
J. Am. Soc. Mass Spectrom. 2022, 33, 1626−1635

terminus (if canonical) or the additional proton on the n-terminus, and a bare oxygen from the original c-terminus moving to the new c-terminus. Oxygen-18 labeling confirmed that the original c-terminus' hydroxy group (or bare oxygen) migrates to the new c-terminus during CID. To the best of our knowledge, no other literature discusses LE+M$^+$. Thus, in an attempt to fill the gap surrounding alkali metal-cationized leucine-enkephalin, SORI-CRAFTI was applied to measure the relative σ of precursor and product ions.

EXPERIMENTAL SECTION

Leucine-enkephalin (LE) was purchased from Sigma-Aldrich as an acetate salt hydrate, lithium chloride was purchased from Fisher Chemical, sodium chloride and cesium chloride were purchases from Mallinckrodt Pharmaceutical, potassium acetate was purchased from J.T. Baker Chemical, rubidium chloride was purchased from Spectrum Chemical, and [2.2.2]-cryptand (222) was obtained from IBC Advanced Technologies, Inc. (American Fork, UT). HPLC-grade methanol, water, and isopropanol (Fisher Chemical) were used to make the electrospray ionization (ESI) solutions. All chemicals were used without further purification.

All LE solutions were dissolved in 50:50 methanol/water. One solution contained LE+Li$^+$, Na$^+$, and K$^+$, while LE+Rb$^+$ and LE+Cs$^+$ each had their own sample solutions. The solutions themselves were approximately equimolar in LE and Li$^+$, while Na$^+$ and K$^+$ were present adventitiously, with total LE concentration being 50 μM. LE+H$^+$ was also present during experiments due to our protic solvent system; no acid was added to the ESI solutions. [2.2.2]-Cryptand solutions were either 50:50 methanol/water or 94:6 isopropanol/water for the reasons detailed below. Samples featured all five alkali metal salts, with excess [2.2.2]-cryptand. ESI samples for use on the FTICR contained 70 μM [2.2.2]-cryptand, 10 μM Li$^+$ (Na$^+$ and K$^+$ again present in the Li$^+$ salt), 10 μM Rb$^+$, and 10 μM Cs$^+$.

All SORI and SORI-CRAFTI experiments were performed on a Bruker Apex 47e Fourier transform ion cyclotron resonance mass spectrometer with a Bruker Infinity trapping cell, and a (heavily modified) Analytica microelectrospray ionization source (Branford, CT).[12] The instrument is controlled by a Predator data acquisition system.[13] A Freiser-style pulsed leak valve[14] was used to introduce collision gas into the trap for ion cooling at the start of the trapping sequence, for SORI-CID, and for CRAFTI measurements. Data were analyzed in Igor Pro 8 (WaveMetrics, Lake Oswego, OR) using custom macros to extract peak widths and amplitudes from the mass spectra.

We performed two types of FTICR-MS experiments to investigate LE+M$^+$. The first was a variable energy sustained off-resonance irradiation collision induced dissociation (SORI-CID) experiment to obtain precursor ion survival (product ion appearance) curves for all five LE+M$^+$ systems. Energy was varied by using a fixed SORI excite amplitude with variable single frequency excite duration. All SORI excite frequencies were 1 kHz off-resonance, though the exact frequency difference was determined during data processing and used to compute relative collisional energy deposition.[15] Argon (Airgas, 99.997% purity) was used as the CID gas, and was pulsed into the trapping cell prior to the SORI event. The pulsed leak valve was pressurized for 500 ms, followed by a 1 s delay to allow the cell pressure to equilibrate. Argon pressure was measured using a cold cathode gauge located about 1 m outside of the trapping cell. Following the SORI event, a 3 s wait event was used to pump argon out of the trapping cell and allow ions to cool and dissociate. While we typically find a 1 s wait time sufficient to pump out the collision gas, a 3 s wait provided more consistent SORI results for LE+Rb$^+$/Cs$^+$.

The second type of experiment was SORI-CRAFTI. SORI was used to dissociate LE+M$^+$. This was accomplished by using a 1 kHz off-resonance single frequency excite that was long enough in time, and strong enough in amplitude, to cause the precursor peak to decrease by approximately 50% compared to initial peak intensity. Prior to the SORI event, argon collision gas was leaked into the trapping cell to a gauge pressure of ~2 $\times$ 10^{-5} mbar. After the SORI sequence, a 1 s wait evacuated the pulsed leak valve system and returned the instrument to base pressure (~9 $\times$ 10^{-9} mbar), and the ions were allowed to cool. The total wait time between SORI and CRAFTI was slightly more than 2 s.

The CRAFTI sequence then started by leaking argon gas into the trapping cell again and using resonant RF excitation for ion detection. The resonant excite was the sum of two single frequency waveforms, designed to excite two ions simultaneously in a strategy known as multi-CRAFTI.[16] Ion-neutral collisions shortened the time domain signal, causing frequency peak broadening. The fwhm of both ion peaks were extracted and used in eq 1 to calculate the two ions' relative σ. Since σ were obtained using multi-CRAFTI, they were directly compared with each other and with σ ratios obtained through computational modeling.

Multi-CRAFTI experiments on 222+M$^+$ were performed as described above, but without the SORI step. SORI-CRAFTI experiments on 222+Cs$^+$ were also performed as described for LE+M$^+$ (Δf = 1 kHz on the high m/z side, ~50% relative precursor peak loss), though the multi-CRAFTI portion was performed by simultaneously exciting 222+Cs$^+$ and 222+K$^+$ instead of a product ion. Additionally, 222+K$^+$ was not SORI activated. In all cases, σ within each experiment were compared by ratio: M$^+$/K$^+$.

An Agilent 6560 ion mobility Q-TOF-MS instrument was used to compare with SORI-CRAFTI. Our 6560 also features an additional counter electrode ("Fragmentor") at the end of the sampling capillary which enables ion acceleration, and high energy collisions with background gas, to cause in-source ion activation,[17] similar to nozzle-skimmer source dissociation.[18] While this upgrade has been used for collision-induced unfolding (CIU) by other research groups,[19] we used it for collision induced dissociation (CID). This setup was used to measure momentum transfer collision integrals (Ω) of precursor and product ions for direct comparison with SORI-CRAFTI results. All IM-MS (and CID-IM-MS) experiments were performed using the Agilent nanoelectrospray source. The instrument was controlled using MassHunter Workstation Data Acquisition (Version B.09.00, Build 9.09044.1 SP1). Nitrogen was used as the drift gas, with the drift tube kept at a pressure of 3.95 Torr. The stepped field method was used to obtain collision Ω measurements for all systems,[20] with the drift voltage varied systematically from 1000 to 1600 V in 100 V steps. Other pertinent instrument parameters are summarized in Table S1. All data were analyzed using MassHunter IM-MS Browser (Version B.08.00). Lastly, sample solutions for use on the Agilent 6560 were approximately 20 μM in LE, with one sample composed of equimolar LE and Li$^+$, while adventitious Na$^+$ and K$^+$ were also

https://doi.org/10.1021/jasms.2c00089
J. Am. Soc. Mass Spectrom. 2022, 33, 1626−1635

present. The other sample contained 10 μM LE, 5 μM Rb^+, and 5 μM Cs^+.

Computational modeling was performed using the Spartan '18 Parallel Suite (Wavefunction, Inc., Irvine, CA). Spartan's conformer distribution algorithm, using the MMFF force field supplied in the computational package (parameters for Rb^+ and Cs^+ were added to the force field),[21] and Monte Carlo searching were used to identify low energy structures for canonical and zwitterionic LE+M^+ and fragments and 222+M^+ systems. Single-point energy calculations were then performed on the resulting MMFF structures at the B3LYP-D3/6-31+G* level of theory for LE+M^+ and fragments and M06-2X/6-31+G* for 222+M^+[22,23] to obtain more accurate energies and Boltzmann weight scoring. The lowest energy conformer was then submitted for full geometry optimization and final energy calculations by the B3LYP-D3/6-311+G**//B3LYP-D3/6-31+G* method for LE+M^+ and by the M06-2X/6-311+G**//M06-2X/6-31+G* method for 222+M^+ to obtain representative structures and to compare canonical and zwitterionic forms (for the LE+M^+ precursor and product ions). For atom types not included in the 6-31+G* or 6-311+G** basis sets, Spartan '18 defaults to LANL2DZ and DEF2-TZVPPD, respectively, each with appropriate pseudopotential. Cross-section prediction was accomplished via the projection approximation (PA)[24] with a Boltzmann-weighted average calculated as described below.

Unlike ion mobility, CRAFTI does not spatially separate ions with the same m/z but different σ. Rather, all like-m/z ions are in the same coherent ion packet, regardless of their σ differences. To account for how different possible conformers contribute to the overall measurement, Boltzmann-weighted average σ are used for comparison with experiment. Modeled σ were obtained using IMoS 1.10c.[24] This was done by submitting all structures generated from Spartan's conformation search for 500-rotation PA calculations in argon, with the argon radius being 188 pm, its accepted van der Waals radius.[25] After extracting the σ values, a Boltzmann distribution was calculated based on the DFT-derived energies described earlier. Cross section ratios (precursor/product) were then calculated for all relevant combinations to facilitate comparison with experimental ratio values. Relative standard deviations, also determined by Boltzmann weighting, of the absolute and ratio cross-section values are less than 1%.

Either the very simple projection approximation (PA) or the somewhat more sophisticated exact hard-sphere scattering (EHSS)[26] method could be used to compute σ values from calculated molecular structures for comparison with CRAFTI. The differences between PA and EHSS results for a given structure are small and comparable to the inherent error in the experimental measurements.[3] Because the PA method is computationally inexpensive compared to EHSS and models the single-collision dephasing conditions expected in CRAFTI, we opted to use the simple PA approach. For comparison with ion mobility results, trajectory method (TM) Ω values were also obtained via IMoS 1.10c. The TM calculations used nitrogen as the collision gas, had nitrogen's quadrupole moment active (parameter qpol in the IMoS.cla file), and used ESP charges calculated from the final *ab initio* energy calculation in Spartan '18. Comparison of different cross-section modeling approaches for the analysis of CRAFTI and IM data will be the subject of another study.

RESULTS AND DISCUSSION

Benchmarking SORI-CRAFTI with LE+H^+. To demonstrate SORI-CRAFTI as an analytical method, CRAFTI experiments were performed on the following pairs (after SORI-CID of LE+H^+): precursor/water loss (m/z 556/538), precursor/b_4 (556/425), precursor/a_4 (556/397), and b_4/a_4 (425/397). All σ ratios were calculated with the precursor in the numerator and the product in the denominator so that ratios are likely to be 1 or larger. CRAFTI (purple bars) and PA (black bars) σ ratios are displayed in Figure 1. The

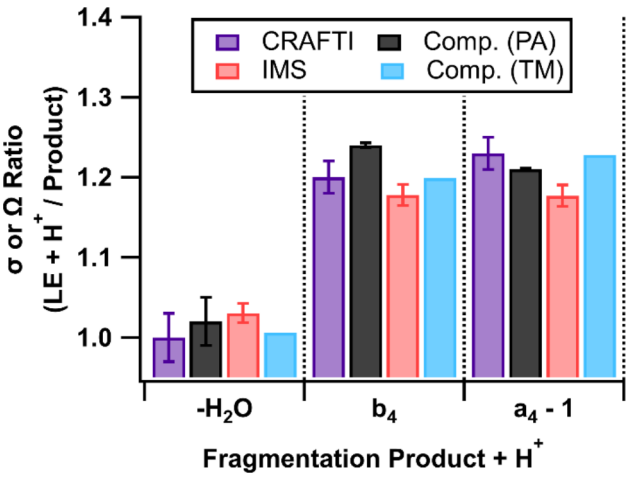

Figure 1. Experimental and computational cross-section ratios (y-axis) for LE+H^+/product. Products used in analysis are listed on the x-axis. Experimental values are ratios based on averages of nine measurements, and error bars are the mean standard deviations. Projection approximation values are ratios of Boltzmann weighted averages, while trajectory method values are from the single lowest energy conformer. Ion mobility values are ratios based on averages of four measurements, and error bars are the propagated mean standard deviations.

precursor and water loss product have a ratio of 1.00 ± 0.03, suggesting that they are approximately the same size. The computational ratio for the water loss product is 1.03, which is a Boltzmann-weighted average of multiple possible dehydration products[27] whose atomic coordinates for the unrefined structures can be found in the Supporting Information (Tables S2−S4). In short, three different possible ions were considered: (1) dehydration at the c-terminus, which results in an oxazolone structure, and (2, 3) cyclic peptides that result from dehydration between the n-terminus and the second or third carbonyl oxygen (numbered from the n-terminus). In all three cases, the positive charge is still associated with the n-terminus.

The precursor/b4 ratio is 1.20 ± 0.02, and the precursor/a4 ratio is 1.23 ± 0.02. While these two ions have statistically different measured σ ratios, as determined by a t test (α = 0.05), computational modeling suggested that the two product structures are similarly sized. A multi-CRAFTI experiment was performed to directly compare the σ ratio of the b_4/a_4 pair. The ratio was 1.01 ± 0.02, which is consistent with the computationally determined value of 1.030 ± 0.002. Computational modeling of these two fragments was based on structures from ref 6, which proposed that the b_4 fragment's primary structure is an oxazolone structure and the a_4 structure involves an imine trans double bond toward the phenylalanine residue.

https://doi.org/10.1021/jasms.2c00089
J. Am. Soc. Mass Spectrom. 2022, 33, 1626−1635

The oxazolone structure causes the b_4 fragment to have a condensed shape compared to the more linear a_4 fragment. These structural differences could account for why the two products are similarly sized even though they differ in mass by 28 u. Reference 6 also proposed, as a secondary structure, an acylium b_4 fragment. The PA b_4(acylium)/a_4 ratio was 1.025 ± 0.001, nearly identical to the b_4(oxazolone)/a_4 PA ratio. Thus, even if the acylium b_4 structure dominated over the oxazolone structure, the cross sections are so similar that current methods cannot distinguish them.

Overall, the σ ratio agreement between CRAFTI and the PA model is qualitatively good, which is encouraging. However, it appears that there is systematic quantitative disagreement between the two, with PA ratios always larger than CRAFTI ratios. Based on the time scale of the experiment, it is possible that either precursor or product ions were still hot and rearranging when the measurement took place. More recent SORI-CRAFTI work featured a varied time-resolved delay between SORI and CRAFTI which revealed that LE+H^+ cools from a large σ to an asymptotic minimum σ within 1.5 s after the SORI excitation is turned off.[28] Since our total ion cooling time was 2 s, it is possible that some portion of the precursor ion population was still hot during the CRAFTI measurement. It is also possible that computationally determined low energy structures do not represent post-SORI activation structures, which could lead to the disagreement.

Figure 1 also shows CID-IM-MS results (red bars) and TM predicted Ω ratios (blue bars). It is unsurprising that precursor/product ratios qualitatively agree since the size relationship between precursor and product ions should be instrument agnostic. Additionally, any effects present in only CRAFTI or IM measurements should be minimized by conversion to ratio, facilitating the comparison. However, quantitative agreement is generally not as good. It is possible that this stems from the fact that ion-neutral collisions in CRAFTI and IMS are fundamentally different. As discussed earlier, CRAFTI involves hard-sphere collisions at tens to hundreds of electronvolts in the center-of-mass frame (dependent on ion m/z). This minimizes the importance of long-range interactions between ion and neutral, such that the result is a measurement of σ.[29,30] On the other hand, drift ion mobility depends on thermal collisions between ion and neutral, which slow the ion's mobility without removing the ion from the packet that traverses the drift tube. This produces momentum transfer collision integrals, Ω. At these lower collision energies, long-range interactions are important,[31] producing Ω that are fundamentally larger than σ and requiring both careful interpretation and more extensive computational modeling.[32] Generally, it appears that comparing general CRAFTI and IM measurements by ratio is a viable way to compare the results.

Another possible explanation for less-than-exact agreement between CRAFTI and IMS ratios arises from the difference in ion activation between SORI-CRAFTI and CID-IMS. SORI causes precursor ions to undergo multiple low energy collisions with neutral gas. The ultimate result is deposition of more energy than the amount deposited via single collisions during on-resonance collision induced dissociation. Generally, the longer the off-resonance RF excitation is applied, the more energy is deposited into the precursor. In our experiments, the off-resonance RF excitation was applied for 50 to 200 ms. Conversely, CID-IMS depends on ion-neutral collisions as ions travel (in the Agilent 6560) from the atmospheric pressure sampling capillary into the front ion funnel, a process measured best in microseconds. Thus, it is possible that SORI-CRAFTI produced significant populations of hot precursor ions, with sufficient energy to rearrange into structures with larger σ than are produced in the CID-IMS process. Additionally, because it takes place in an FTICR-MS, SORI-CRAFTI allows for longer designated wait periods (2 s in our experiments) between activation and measurement than CID-IMS does (1 ms, where the wait period is the result of ion accumulation in the trapping funnel, rather than a dedicated cooling period). This could result in product ions cooling to different kinetic minima that differ in size. Taken together, the activation energy and wait period differences could result in different precursor and product ion populations that differ in size

We note that a similar study, performed in 2008, also used drift ion mobility CID-IMS to study LE+H^+ and the b_4 and a_4 fragments.[8] A unique highlight of that study is the triple drift tube design which allowed greater product ion separation than was possible on our Agilent 6560. The greater separation revealed that the total a_4 product ion population was composed of three distinct subpopulations. Using ref 8's labeling and nomenclature, these subpopulations were (I) a cyclic structure, (II) a cis-imine N-terminal protonated structure, and (III) a trans-imine N-terminal protonated structure, with (estimated by us) precursor/product ratios of (I) 1.24, (II) 1.20, and (III) 1.13. These ratios are in good agreement with what we determined by CRAFTI (1.23) and IMS (1.17). Given that the CRAFTI measurements agree better with I and II while IMS agrees better with II and III, it is possible that each instrument sampled different ion populations due to the time scales available after the collisional activation step and prior to the measurement step. The lone exception for excellent agreement with CRAFTI is product III, which, ironically, was the ion structure we used for modeling purposes. Interestingly, our modeled PA value of 1.28 is much higher than the value of 1.13 (TM) from ref 8, despite both studies using similar (not identical) starting structures. This may be due to differences in how low energy conformers were identified. As described, we used Monte Carlo conformational searching driven by MMFF to identify low energy conformers, while ref 8 used structures identified in ref 6 which were found using molecular dynamics and the Amber force field. Despite that exception, CRAFTI, in-house CID-IMS, and previous CID-IMS-IMS-IMS, reach similar conclusions about the Ω relationship of LE+H^+ and the a_4 product ion.

The 2008 study also analyzed the b_4 ion population and concluded that it included cyclic and oxazolone subpopulations, with (estimated by us) ratios of 1.22 and 1.18, respectively. These ratios are also in good agreement with our CRAFTI value of 1.20.

SORI and SORI-CRAFTI Analysis of LE+M^+. Taking lessons learned from benchmarking experiments, LE+M^+ (M^+ = Li^+, Na^+, K^+, Rb^+, and Cs^+) systems were analyzed by SORI and SORI-CRAFTI. As pointed out earlier, LE+Li^+/Na^+/K^+ were analyzed by tandem mass spectrometry in the late 1980s[10,33] and were found to primarily dissociate into b_n+17+M^+ fragments. For this project, SORI results were used to guide the targeted SORI-CRAFTI experiments.

SORI Results. As described previously, we performed energy-resolved SORI experiments to obtain precursor ion disappearance and product ion appearance curves for all five LE+M^+ precursors. This was done to identify which products were favored and to guide SORI-CRAFTI experiments. Figure

https://doi.org/10.1021/jasms.2c00089
J. Am. Soc. Mass Spectrom. 2022, 33, 1626−1635

S1 contains six plots summarizing the results. Table S5 lists all observed product ions from SORI experiments for each precursor ion.

As is typical of peptides, multiple dissociation pathways were observed for all LE+M^+ precursors. The favored pathway for LE+Li^+/Na^+/K^+ resulted in formation of the b_4+17+M^+ product. Less favored pathways resulted in the LE+M^+-H_2O, b_4+M^+, a_4+M^+, and b_3+17+M^+ products. Collisional activation of LE+K^+ also resulted in formation of the c_3+K^+ product. Additionally, several less-favored pathways resulted in other small molecule (CO, NH_3, CO_2, etc.) losses. The favored pathway for LE+Rb^+ was Rb^+ loss, though another pathway also led to the b_4+17+Rb^+ product. The only observed dissociation pathway for LE+Cs^+ was Cs^+ loss.

The fact that multiple products arose from small molecule (H_2O, CO, NH_3, CO_2) loss suggests that all, or some portion, of the precursor peptide population is present as zwitterions, because several of these products can be lost from the n-terminus (NH_3) and c-terminus (CO, CO_2) of zwitterionic precursors. It is also possible that the peptide is present in its canonical form, but a mobile proton from the c-terminal hydroxy group migrates to the n-terminus during collisional activation, which then leads to ammonia or carbon dioxide loss. However, this may be difficult to confirm without spectroscopic measurements such as IRMPD.

The relative SORI-CID precursor dissociation energies are compared in Figure S1(F) by plotting all the precursor survival yield curves together. These are then compared based on their energies at the 50% survival yield (SY50) point. The SY50 for each LE+M^+ is greater than the SY50 for LE+H^+, as was recently demonstrated for various peptide+Na^+ systems.[34] This could be due to the metal cation affording stability to the peptide that does not occur when the n-terminus is protonated (and is 1+ charged overall).

Many, though not all, dissociation products observed as a result of SORI-CID were also observed following in-source CID in the Agilent 6560. Specifically, SORI-CID of LE+M^+ resulted in 45 total quantifiable product ions while in-source CID (Agilent 6560) resulted in seven quantifiable product ions. The difference in total product ions quantified by each strategy is likely related, again, to the difference between SORI-CID in the FTICR and in-source CID in the IMS-qTOF, the amount of energy deposited through ion-neutral collisions through each strategy, and the amount of time for postactivation dissociation and cooling.

SORI-CRAFTI Results. Figure 2 shows σ ratios for LE+Li^+ (A), Na^+ (B), and K^+ (C) precursors and selected product ions as obtained by SORI-CRAFTI (left, purple bars) and CID-IMS (right, red bars). LE+Rb^+ is not included since the σ ratio obtained via SORI-CRAFTI (LE+Rb^+/b_4+17+Rb^+) did not have a counterpart obtained via CID-IMS. LE+Cs^+ is not included because neither SORI nor traditional CID resulted in peptide dissociation.

The first thing to note in Figure 2 is the excellent qualitative agreement between CRAFTI ratios and IMS ratios. The only systems for which qualitative agreement is poor is for the smallest product ions (b_3+17 for Li^+ and Na^+, and c_3 for K^+), which are the lowest m/z ions detected, the smallest in terms of cross-section value, and produce the lowest intensity signal of all product ions measured in this study. The disagreement likely arises more from inaccuracies in the CRAFTI measurement than from IM. A fundamental shortcoming of CRAFTI is its reliance on initial ion signal, as σ is measured based on the

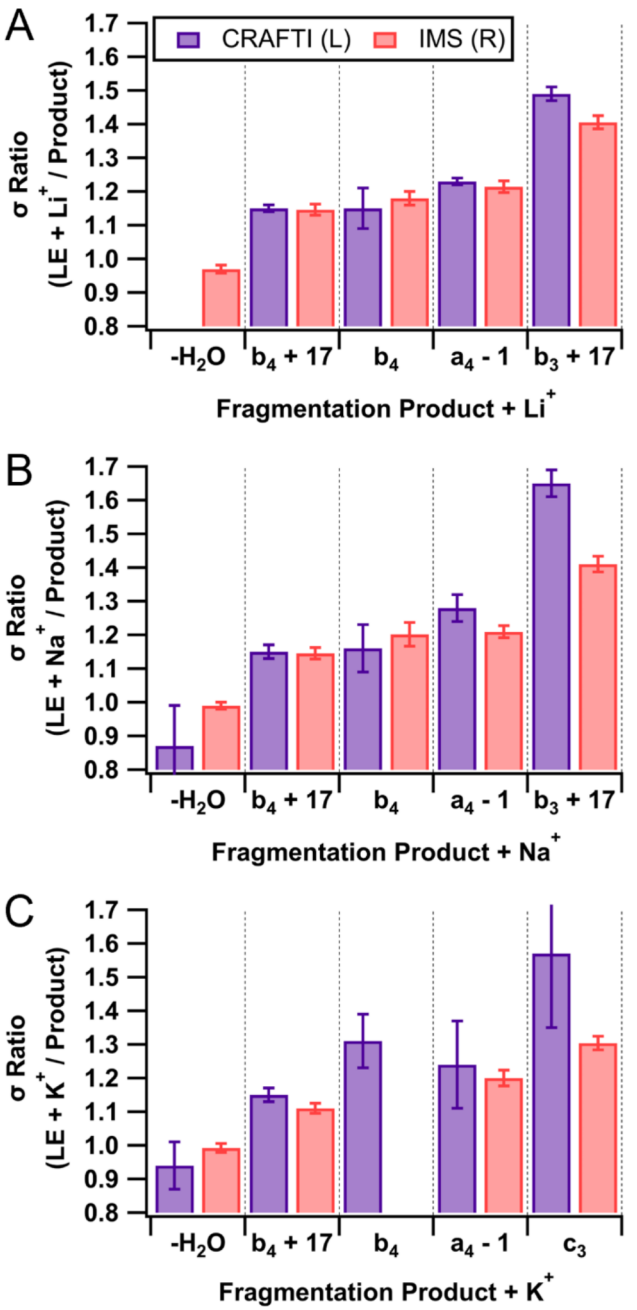

Figure 2. Multi-CRAFTI ratios (y-axis) for LE + Li^+/Na^+/K^+/Rb^+ and their respective products (x-axis). CRAFTI ratios are averages of 7−9 measurements, while IMS ratios are averages of four measurements. In each case, error bars are one standard deviation of the mean.

rate at which ions are removed from coherent ion packets. Thus, weak initial ion signal results in poor CRAFTI results, such as increased %RSD, which could result in a wider quantitative gap between the CRAFTI and IMS ratios.

A second thing to note in Figure 2 is the lack of computationally modeled ratios, as were present in Figure 1 for LE+H^+. Modeled structures used for LE+H^+ and its fragments were based on structures well characterized by gas-phase action spectroscopy, as discussed above. This facilitated cross-section prediction, and comparison with experimental results. On the other hand, structures for LE+M^+ and the resulting fragments are based on accurate m/z values, chemical

https://doi.org/10.1021/jasms.2c00089
J. Am. Soc. Mass Spectrom. 2022, 33, 1626−1635

intuition, and MMFF-driven Monte Carlo conformational searching. Since each metalated precursor, and the b_n+17+M^+ products, can be present in their canonical or zwitterionic forms, modeling and analysis were not straightforward. Despite extensive efforts, described below, neither the precursors, nor the b_n+17+M^+ products, could confidently be identified as canonical or zwitterionic. Thus, modeled ratios are not included for comparison with experimental results.

The third thing to note in Figure 2 is the fact that b_4+K^+ was not observed using CID-IMS. It is possible that b_4+K^+ results from further dissociation of a different product+K^+ ion such that additional time after activation is required for the former's formation. As discussed previously, the FTICR affords much longer 'wait' times than the IM-MS, which could account for b_4+K^+'s presence in the FTICR but not the IMS-ToF.

Last, it is interesting to note that ratio values for identical product ions are highly similar, regardless of cation identity and size. This suggests that each product ion coordinates to the metal cation in similar ways, and that the physical cation size plays little role in the physical size of the peptide+M^+ structure.

Efforts to characterize precursors and products as either canonical or zwitterionic involved comparison of experimental ratios with computational ratios and high-level *ab initio* calculations for relative energy comparisons.

Comparison of Experimental and Computationally Predicted Ratios. As each precursor, and the b_n+17 products, have canonical or zwitterionic forms, four different computationally predicted ratios were considered. These were: [canonical precursor]/[canonical fragment], [zwitterionic precursor]/[zwitterionic fragment], [canonical precursor]/[zwitterionic fragment], and [zwitterionic precursor]/[canonical fragment]. Comparison of each of these with the experimentally measured ratio revealed multiple different possibilities either in agreement, or very close in agreement, or poor agreement, with experiment (Tables S6 and S7). Additionally, there was no consistent trend across precursors and products based on metal cation identity. Ultimately, σ values did not clearly distinguish between the possibilities.

***Ab Initio* Calculations for Relative Energy Comparison.** To clear up whether precursors and product ions are present in their canonical or zwitterionic forms, we turned to higher level DFT calculations to determine which peptide form was favored in the gas phase. These calculations revealed that canonical and zwitterionic lithium and sodium precursors are within 1 kJ/mol of each other, potassium precursors are within 14 kJ/mol of each other (with zwitterionic being favored), and rubidium precursors are within 7 kJ/mol of each other (with canonical favored). Thus, our data suggest that both canonical and zwitterionic precursor forms may be present in the gas phase for all metals. Similar calculations for the b_n+17+M^+ products revealed that the canonical form is favored by at least 24 kJ/mol over the zwitterionic forms. The only system excepted from this trend is b_3+17+Na^+, whose canonical form is favored by just 2 kJ/mol. Again, based on these results, no definite conclusions could be reached about canonical versus zwitterionic precursor and product ions. Thus, computationally predicted ratios were not included in Figure 2.

While it is disappointing that the complementary approach of cross-section measurement, tandem MS, and high-level DFT calculations was insufficient to confidently identify LE+M^+ precursors and b_n+17+M^+ product ions as canonical or zwitterionic, this result is unsurprising. This complementary strategy cannot elucidate fine structural features to the same extent as condensed-phase methods such as NMR and X-ray crystallography or gas-phase methods like action spectroscopy. In the case of investigating gas-phase chemistry, IRMPD may be a better option to definitively identify precursor and product ions as either canonical, zwitterionic, or a mixture of both.

Overall, SORI-CRAFTI and CID-IMS were able to quantify σ and Ω ratios for several precursor/product pairs, which can facilitate peptide identification through complementary information acquired in the course of each experiment, namely: m/z, σ or Ω, and fragmentation pattern. In this regard, SORI-CRAFTI, like CID-IMS, may be a useful tool for molecular structure identification.

[2.2.2]-Cryptand and Alkali Metal Cations. Since SORI-CRAFTI was unable to determine whether metalated LE was present in its canonical or zwitterionic form, we turned our attention to a different system to show how SORI-CRAFTI could be used to probe gas-phase ion structure. We chose [2.2.2]-cryptand, a macrocyclic host capable of binding metal cations through its six ether oxygens (Figure 3 inset).[35] Of the

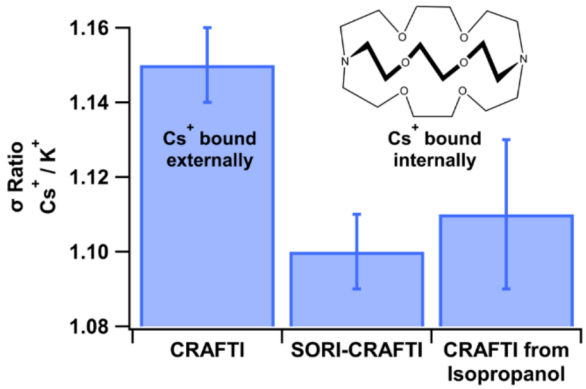

Figure 3. 222+Cs^+/222+K^+ average σ ratios measured by two different techniques and two different solvent systems. Error bars are the mean standard deviations.

alkali metal cations, lithium through rubidium are all small enough to fit within [2.2.2]-cryptand, forming an alkali metal cryptate. However, cesium has been shown to bind both internally and externally to [2.2.2]-cryptand, depending on solvent, with aqueous solvents favoring external binding and less polar solvents favoring internal binding.[36] Initial multi-CRAFTI results, from a 50/50 methanol/water electrospray solution, comparing 222+M^+ and 222+K^+ (SI Figure S2) showed a large jump in ratio value (M^+/K^+) between Rb^+ and Cs^+, indicative that Cs^+ is bound externally to [2.2.2]-cryptand. This result has been consistent over many years in our lab, regardless of which researcher makes the measurement.

Using a fresh electrospray sample (50:50 water/methanol) of [2.2.2]-cryptand and cesium chloride (sodium and potassium were present due to contamination), we repeated multi-CRAFTI measurements for 222+K^+ and 222+Cs^+, which returned a ratio in agreement with previous values (1.15 ± 0.01). We then attempted to anneal 222+Cs^+ to an internally bound conformation using SORI. After SORI activation of 222+Cs^+ to induce ~50% relative peak intensity loss, relative σ values for 222+K^+ and 222+Cs^+ were again obtained by multi-CRAFTI. The ratio decreased to 1.10 ± 0.01 (Figure 3, middle bar), indicating a −4.5% change in 222+Cs^+ collision cross

https://doi.org/10.1021/jasms.2c00089
J. Am. Soc. Mass Spectrom. 2022, 33, 1626−1635

section. A student t test comparing the two multi-CRAFTI ratios confirmed that the mean values are statistically different. This result strongly suggested that either (1) 222+Cs^+ (external) was activated and annealed to 222+Cs^+ (internal) or (2) the initial ion population was composed of both internally and externally bound 222+Cs^+, and SORI activation caused 222+Cs^+ (external) to dissociate, leaving the remaining population enriched in the internally bound complex.

To test the interpretation that the resultant 222+Cs^+ population featured Cs^+ bound internally, we performed the same multi-CRAFTI measurement using a 6:94 water/isopropanol solvent system. This is based on NMR evidence which showed that solvents with similar dielectric constants to isopropanol resulted in 222+Cs^+ (internal), while solvents with dielectric constants similar to water resulted in 222+Cs^+ (external).[37] The multi-CRAFTI ratio for the isopropanol solution was 1.11 ± 0.02 (Figure 3) in statistical agreement (t test, α = 0.05) with the SORI-CRAFTI ratio and statistically different (t test, α = 0.05) from the CRAFTI ratio obtained without activation. While we could not confirm whether SORI heating caused annealing to convert Cs^+ (external) to Cs^+ (internal), or whether dissociation of Cs^+ (external) to leave behind a population enriched in Cs^+ (internal), it is clear that SORI induced a net structural change in the ion population, which was measurable by CRAFTI.

Evaluation of SORI-CRAFTI and CID-IMS. Table 1 summarizes how many precursor/product pairs were measured

Table 1. Number of Product Ions Whose σ or Ω was Measured by Each Method

precursor	SORI-CRAFTI	CID-IMS
LE+H^+	3	9
LE+Li^+	5	11
LE+Na^+	6	10
LE+K^+	6	6
LE+Rb^+	1	0
LE+Cs^+	0	0
total	21	36
acquisition time	31.5 h	14 min

for each precursor ion by each method. Interestingly, although SORI produced a wider range of fragment ions (a total of 53, including those from LE+H^+) than were seen using in-source CID (a total of 37, including those from LE+H^+), collision cross sections for more fragment ions were measurable using IMS than we were able to measure using CRAFTI. It is impressive to note that CID-IMS measured nearly double the number of precursor/product ion pairs, in a fraction of the time, compared to SORI-CRAFTI. A few differences in experimental design likely led to this result. In regard to data acquisition rate, SORI and CRAFTI are targeted FTICR methods, which results in activation of one precursor species, followed by σ measurement of the precursor and one product ion. By its nature, that is a slow process. Additionally, in this data acquisition setup, SORI requires collision gas introduction prior to the SORI event sequence, then collision gas removal prior to reintroducing collision gas at lower pressures for the CRAFTI sequence. The pump-up and pump-down portions result in experimental time lengths approaching 10 s per scan, which quickly becomes 50 to 100 s when multiple scans are averaged. Since CRAFTI requires data collection at multiple pressures to form a single replicate, that one replicate, of only 2 ions, takes approximately 10 min if six pressure points are used. Thus, for statistically relevant data of three or more replicates (nine replicates as presented here), SORI-CRAFTI experiments require 30 (90) minutes to complete. By comparison, CID-IMS is a nontargeted (all ions) analytical method. As ions were directly infused via nanoESI, they traveled more or less together through the instrument's source region which is where collisional activation took place. Thus, all precursor ions present in each sample were activated simultaneously, resulting in broad product ion formation. All ions then traveled through the instrument's drift region prior to detection in the time-of-flight segment. In our CID-IMS method, one replicate, containing all 36 ions, was completed in 3.5 min, and four replicates were completed in 14 min. Taken together, the number of ions quantified and the rapidity of data acquisition, makes CID-IMS the obvious choice for omics-type workflows.

As discussed above, CRAFTI requires as strong an initial signal intensity as possible since ions will be lost from the ion packet through ion-neutral collisions and as the pressure increases. As mentioned above, six different pressure points were used, which covered 1 order of magnitude pressure range. The final pressure caused such low signal intensity that averaging of 10 scans was required to produce quantifiable signal peaks. For those product ions whose relative signal intensity is weak to begin with (for example, a nonfavored dissociation pathway), the signal peak is generally lost in the noise prior to reaching the maximum pressure required for σ measurement. This prevents measuring the σ ratio for that precursor/product pair. In contrast, drift ion mobility does not depend on single collision ion removal from the ion group, nor does it require various pressures to measure Ω, so there is minimal pressure-induced ion loss, preserving signal intensity. Additionally, the Agilent 6560 is designed for sensitivity, possessing multiple ion funnels that refocus the ion beam and prevent ion loss.[38,39] Thus, product ions whose relative signal intensity may be weak in the FTICR are easily detected by the Agilent 6560.

These differences between SORI-CRAFTI and CID-IMS present opportunities to further improve CRAFTI. First, it is possible to use a form of broadband excitation to collisionally activate ions in the FTICR, making activation less targeted.[40] Second, it may be possible to perform CRAFTI measurements at a single high pressure instead of over a range of pressures, which would simplify and speed up data acquisition. Finally, it may be possible to use broadband RF excitation for detection instead of waveforms that are either a single frequency or the sum of two frequencies. This would also simplify and speed up data acquisition.

Despite these drawbacks, and the need to improve SORI-CRAFTI to make it more generally useful, the technique was useful for studying internally and externally bound 222+Cs^+. When electrosprayed from water:methanol, which should have produced externally bound Cs^+, SORI heating of the externally bound Cs^+ complex was sufficient to facilitate annealing to an internally bound Cs^+ complex. Subsequent CRAFTI measurement then confirmed this change. This suggests that energy-resolved SORI-CRAFTI might be used to produce an annealing curve based on σ value or ratio.

Additionally, CRAFTI itself remains an excellent tool for investigating gas-phase ion chemistry as demonstrated recently.[41] That work examined fragile host/guest systems which dissociated at very low relative collision energies. Multi-CRAFTI was key to characterizing how the guest ions were

https://doi.org/10.1021/jasms.2c00089
J. Am. Soc. Mass Spectrom. 2022, 33, 1626−1635

bound to the host. Attempts to replicate that work on the Agilent 6560 were unsuccessful because these fragile complexes were not observed using the Agilent instrument. The paper concludes that the fragile host/guest systems likely dissociated through multiple low energy collisions prior to (or during) mobility separation. This did not happen in the FTICR since it is maintained at ultrahigh vacuum for a majority of the experiment, preventing multiple low energy collisions from occurring prior to σ measurement.

CONCLUSION

An FTICR-MS is a formidable gas-phase processing laboratory capable of ion activation and high-resolution, accurate mass measurements. To its repertoire, CRAFTI adds the ability to measure σ. This aids investigation of the connection between gas-phase structure and chemistry. When CRAFTI is combined with SORI (SORI-CRAFTI), gas-phase structures of precursor and selected product ions can be studied together in the same experiment. While this targeted approach has potential for ion chemistry or -omics studies, it does require more time to implement when compared with IM-MS instruments that offer premeasurement ion activation capabilities. Additionally, SORI can also be used to cause ion structural changes, which are then reflected in comparative CRAFTI measurements.

ASSOCIATED CONTENT

Supporting Information

The Supporting Information is available free of charge at https://pubs.acs.org/doi/10.1021/jasms.2c00089.

Agilent 6560 IM-q-TOF parameters; atomic coordinates for computed leucine enkephalin dehydration products; collision-induced dissociation plots for protonated and metalated leucine enkephalin; listing of product ions observed using SORI-CID and CID-IMS; tables of precursor/product ratios from SORI-CRAFTI, projection approximation calculations, IM-MS, and trajectory method calculations; absolute collision cross-section IM-MS measurements for protonated and metalated leucine enkephalin; plot of multi-CRAFTI results for cryptand 222+M^+/222+K^+ (PDF)

AUTHOR INFORMATION

Corresponding Author

David V. Dearden − *Department of Chemistry and Biochemistry, Brigham Young University, Provo, Utah 84602-1030, United States;* orcid.org/0000-0003-0899-7776; Phone: 801-422-2355; Email: dvd@chem.byu.edu

Authors

Andrew J. Arslanian − *Department of Chemistry and Biochemistry, Brigham Young University, Provo, Utah 84602-1030, United States*

Noah Mismash − *Department of Chemistry and Biochemistry, Brigham Young University, Provo, Utah 84602-1030, United States*

Complete contact information is available at: https://pubs.acs.org/10.1021/jasms.2c00089

Notes

The authors declare no competing financial interest.

ACKNOWLEDGMENTS

All authors thank the National Science Foundation for support of this work (CHE-1904838), and the BYU College of Physical and Mathematical Sciences for undergraduate research funds. AJA also thanks the Roland K. Robins, Rex and Marcia A. Goates, and Loren and Maurine F. Bryner families for graciously funding graduate research fellowships awarded to him by BYU's Department of Chemistry and Biochemistry.

REFERENCES

(1) Yang, F.; Voelkel, J. E.; Dearden, D. V. Collision Cross Sectional Areas from Analysis of Fourier Transform Ion Cyclotron Resonance Line Width: A New Method for Characterizing Molecular Structure. *Anal. Chem.* **2012**, *84*, 4851−4857.

(2) Yang, F.; Jones, C. A.; Dearden, D. V. Effects of Kinetic Energy and Collision Gas on Measurement of Cross Sections by Fourier Transform Ion Cyclotron Resonance Mass Spectrometry. *Int. J. Mass Spectrom.* **2015**, *378*, 143−150.

(3) Anupriya; Gustafson, E.; Mortensen, D. N.; Dearden, D. V. Quantitative Collision Cross-Sections from FTICR Linewidth Measurements: Improvements in Theory and Experiment. *J. Am. Soc. Mass Spectrom.* **2018**, *29*, 251−259.

(4) Sievers, H. L.; Grützmacher, H.-F.; Caravatti, P. The geometrical factor of infinitely long cylindrical ICR cells for collision energy-resolved mass spectrometry: appearance energies of EI_2^+ (E = P, As, Sb, and Bi) from collision-induced dissociation of EI_3^+ and $[EI{\bullet}ligand]^+$ complexes. *Int. J. Mass Spectrom. Ion Proc.* **1996**, *157/158*, 233−247.

(5) Sztáray, J.; Memboeuf, A.; Drahos, L.; Vékey, K. Leucine enkephalin-A mass spectrometry standard. *Mass Spectrom. Rev.* **2011**, *30*, 298−320.

(6) Polfer, N. C.; Oomens, J.; Suhai, S.; Paizs, B. Infrared Spectroscopy and Theoretical Studies on Gas-Phase Protonated Leu-enkephalin and Its Fragments: Direct Experimental Evidence for the Mobile Proton. *J. Am. Chem. Soc.* **2007**, *129*, 5887−5897.

(7) Burke, N. L.; Redwine, J. G.; Dean, J. C.; McLuckey, S. A.; Zwier, T. S. UV and IR spectroscopy of cold protonated leucine enkephalin. *Int. J. Mass Spectrom.* **2015**, *378*, 196−205.

(8) Polfer, N. C.; Bohrer, B. C.; Plasencia, M. D.; Paizs, B.; Clemmer, D. E. On the Dynamics of Fragment Isomerization in Collision-Induced Dissociation of Peptides. *J. Phys. Chem. A* **2008**, *112*, 1286−1293.

(9) Bleiholder, C.; Dupuis, N. F.; Wyttenbach, T.; Bowers, M. T. Ion mobility-mass spectrometry reveals a conformational conversion from random assembly to β-sheet in amyloid fibril formation. *Nat. Chem.* **2011**, *3*, 172−177.

(10) Tang, X.; Ens, W.; Standing, K. G.; Westmore, J. B. Daughter ion mass spectra from cationized molecules of small oligopeptides in a reflecting time-of-flight mass spectrometer. *Anal. Chem.* **1988**, *60*, 1791−1799.

(11) Grese, R. P.; Cerny, R. L.; Gross, M. L. Metal ion-peptide interactions in the gas phase: a tandem mass spectrometry study of alkali metal cationized peptides. *J. Am. Chem. Soc.* **1989**, *111*, 2835−2842.

(12) Wigger, M.; Nawrocki, J. P.; Watson, C. H.; Eyler, J. R.; Benner, S. A. Assessing Enzyme Substrate Specificity Using Combinatorial Libraries and Electrospray Ionization-Fourier Transform Ion Cyclotron Resonance Mass Spectrometry. *Rapid Commun. Mass Spectrom.* **1997**, *11*, 1749−1752.

(13) Blakney, G. T.; Hendrickson, C. L.; Marshall, A. G. Predator data station: A fast data acquisition system for advanced FT-ICR MS experiments. *Int. J. Mass Spectrom.* **2011**, *306*, 246−252.

(14) Jiao, C. Q.; Ranatunga, D. R. A.; Vaughn, W. E.; Freiser, B. S. A Pulsed-Leak Valve for Use with Ion Trapping Mass Spectrometers. *J. Am. Soc. Mass. Spectrom.* **1996**, *7*, 118−122.

(15) Zhang, H.; Ferrell, T. A.; Asplund, M. C.; Dearden, D. V. Molecular Beads on a Charged Molecular String: α,ω-Alkyldiammo-

nium Complexes of Cucurbit[6]uril in the Gas Phase. *Int. J. Mass Spectrom.* **2007**, *265*, 187−196.
(16) Pope, B. L.; Joaquin, D.; Hickey, J. T.; Mismash, N.; Heravi, T.; Shrestha, J.; Arslanian, A. J.; Anupriya; Mortensen, D. N.; Dearden, D. V. Multi-CRAFTI: Relative Collision Cross Sections from Fourier Transform Ion Cyclotron Resonance Mass Spectrometric Line Width Measurements. *J. Am. Soc. Mass. Spectrom.* **2022**, *33*, 131−140.
(17) Fjeldsted, J. C. Personal Correspondence.
(18) Loo, J. A.; Udseth, H. R.; Smith, R. D.; Futrell, J. H. Collisional effects on the charge distribution of ions from large molecules, formed by electrospray-ionization mass spectrometry. *Rapid Commun. Mass Spectrom.* **1988**, *2*, 207−210.
(19) Vallejo, D. D.; Polasky, D. A.; Kurulugama, R. T.; Eschweiler, J. D.; Fjeldsted, J. C.; Ruotolo, B. T. A Modified Drift Tube Ion Mobility-Mass Spectrometer for Charge-Multiplexed Collision-Induced Unfolding. *Anal. Chem.* **2019**, *91*, 8137−8146.
(20) McLean, J. A.; Schultz, J. A.; Woods, A. S. *Ion Mobility-Mass Spectrometry*; John Wiley & Sons, Inc., 2012; pp 411−439.
(21) Hickenlooper, S. M.; Harper, C. C.; Pope, B. L.; Mortensen, D. N.; Dearden, D. V. Barriers for Extrusion of a Guest from the Interior Binding Cavity of a Host: Gas Phase Experimental and Computational Results for Ion-Capped Decamethylcucurbit[5]uril Complexes. *J. Phys. Chem. A* **2018**, *122*, 9224−9232.
(22) Jami-Alahmadi, Y.; Linford, B. D.; Fridgen, T. D. Distinguishing Isomeric Peptides: The Unimolecular Reactivity and Structures of (LeuPro)M + and (ProLeu)M + (M = Alkali Metal). *J. Phys. Chem. B* **2016**, *120*, 13039−13046.
(23) Cheng, R.; Loire, E.; Martens, J.; Fridgen, T. D. An IRMPD spectroscopic and computational study of protonated guanine-containing mismatched base pairs in the gas phase. *Phys. Chem. Chem. Phys.* **2020**, *22*, 2999−3007.
(24) Larriba, C.; Hogan, C. J. Free molecular collision cross section calculation methods for nanoparticles and complex ions with energy accommodation. *J. Comput. Phys.* **2013**, *251*, 344−363.
(25) Mantina, M.; Chamberlin, A. C.; Valero, R.; Cramer, C. J.; Truhlar, D. G. Consistent van der Waals Radii for the Whole Main Group. *J. Phys. Chem. A* **2009**, *113*, 5806−5812.
(26) Shvartsburg, A. A.; Jarrold, M. F. An exact hard-spheres scattering model for the mobilities of polyatomic ions. *Chem. Phys. Lett.* **1996**, *261*, 86−91.
(27) Ballard, K. D.; Gaskell, S. J. Dehydration of peptide [M + H]+ ions in the gas phase. *J. Am. Soc. Mass Spectrom.* **1993**, *4*, 477−481.
(28) Arslanian, A. J.; Porter, S.; Dearden, D. V. Time-resolved Ion Structural Changes by Cross-section Measurement in a Fourier Transform Ion Cyclotron Resonance Mass Spectrometer. *69th ASMS Conference on Mass Spectrometry and Allied Topics*, Philadelphia, PA, 2021.
(29) Shirts, R. B. Collision Theory and Reaction Dynamics. In *Gaseous Ion Chemistry and Mass Spectrometry*, Futrell, J. H., Ed.; John Wiley & Sons, 1986; pp 25−57.
(30) Su, T.; Bowers, M. T. Classical Ion−Molecule Collision Theory. In *Gas Phase Ion Chemistry*, Bowers, M. T., Ed.; Vol. *1*; Academic, 1979; pp 83−118.
(31) Wyttenbach, T.; Bleiholder, C.; Bowers, M. T. Factors Contributing to the Collision Cross Section of Polyatomic Ions in the Kilodalton to Gigadalton Range: Application to Ion Mobility Measurements. *Anal. Chem.* **2013**, *85*, 2191−2199.
(32) Naylor, C. N.; Clowers, B. H. Reevaluating the Role of Polarizability in Ion Mobility Spectrometry. *J. Am. Soc. Mass Spectrom.* **2021**, *32*, 618−627.
(33) Leary, J. A.; Williams, T. D.; Bott, G. Strategy for sequencing peptides as mono- and dilithiated adducts using a hybrid tandem mass spectrometer. *Rapid Commun. Mass Spectrom.* **1989**, *3*, 192−196.
(34) Logerot, E.; Enjalbal, C. Dissociation Pattern of Sodiated Amide Peptides as a Tool for De Novo Sequencing. *J. Am. Soc. Mass Spectrom.* **2020**, *31*, 2328−2337.
(35) Lehn, J.-M.; Sauvage, J.-P. [2]-Cryptates: Stability and Selectivity of Alkali and Alkaline-Earth Macrobicyclic Complexes. *J. Am. Chem. Soc.* **1975**, *97*, 6700−6707.
(36) Mei, E.; Popov, A. I.; Dye, J. L. Cesium-133 Nuclear Magnetic Resonance Study of Complexation by Cryptand C222 in Various Solvents: Evidence for Exclusive and Inclusive Complexes. *J. Am. Chem. Soc.* **1977**, *99*, 6532−6536.
(37) Mei, E.; Liu, L.; Dye, J. L.; Popov, A. I. Determination of Stability Constants of Cesium [2]-Cryptand Complexes in Non-aqueous Solvents by Cesium-133 NMR. *J. Solution Chem.* **1977**, *6*, 771−778.
(38) Baker, E. S.; Clowers, B. H.; Li, F.; Tang, K.; Tolmachev, A. V.; Prior, D. C.; Belov, M. E.; Smith, R. D. Ion mobility spectrometry—mass spectrometry performance using electrodynamic ion funnels and elevated drift gas pressures. *J. Am. Soc. Mass Spectrom.* **2007**, *18*, 1176−1187.
(39) May, J. C.; Goodwin, C. R.; Lareau, N. M.; Leaptrot, K. L.; Morris, C. B.; Kurulugama, R. T.; Mordehai, A.; Klein, C.; Barry, W.; Darland, E.; et al. Conformational Ordering of Biomolecules in the Gas Phase: Nitrogen Collision Cross Sections Measured on a Prototype High Resolution Drift Tube Ion Mobility-Mass Spectrometer. *Anal. Chem.* **2014**, *86*, 2107−2116.
(40) Guan, S.; Marshall, A. G. Stored waveform inverse Fourier transform (SWIFT) ion excitation in trapped-ion mass spectometry: Theory and applications. *Int. J. Mass Spectrom. Ion Process.* **1996**, *157−158*, 5−37.
(41) Heravi, T.; Shen, J.; Johnson, S.; Asplund, M. C.; Dearden, D. V. Halide Size-Selective Binding by Cucurbit[5]uril—Alkali Cation Complexes in the Gas Phase. *J. Phys. Chem. A* **2021**, *125*, 7803−7812.

https://doi.org/10.1021/jasms.2c00089
J. Am. Soc. Mass Spectrom. 2022, 33, 1626−1635